This is a repository copy of *Photoreflectance and surface photovoltage spectroscopy of beryllium-doped GaAs/AlAs multiple quantum wells* .

White Rose Research Online URL for this paper:
http://eprints.whiterose.ac.uk/1694/

Photoreflectance and surface photovoltage spectroscopy of beryllium-doped GaAs/AlAs multiple quantum wells

B. Čechavičius and J. Kavaliauskas[a)]
Semiconductor Physics Institute, A. Goštauto Street 11, LT-01108 Vilnius, Lithuania

G. Krivaitė, D. Seliuta, and G. Valušis
*Semiconductor Physics Institute, A. Goštauto Street 11, LT-01108 Vilnius, Lithuania
and Vilnius Gediminas' Technical University, Sauletekio Avenue 11, LT-10223 Vilnius, Lithuania*

M. P. Halsall
Department of Electronics and Electrical Engineering, University of Manchester, P.O. Box 88, Manchester M60 1QD, United Kingdom

M. J. Steer
Department of Electronic and Electrical Engineering, University of Sheffield, Mappin Street, Sheffield S1 3JD, United Kingdom

P. Harrison
Institute of Microwaves and Photonics, School of Electronic and Electrical Engineering, University of Leeds, Leeds LS2 9JT, United Kingdom

We present an optical study of beryllium δ-doped GaAs/AlAs multiple quantum well (QW) structures designed for sensing terahertz (THz) radiation. Photoreflectance (PR), surface photovoltage (SPV), and wavelength-modulated differential surface photovoltage (DSPV) spectra were measured in the structures with QW widths ranging from 3 to 20 nm and doping densities from 2×10^{10} to 5×10^{12} cm^{-2} at room temperature. The PR spectra displayed Franz-Keldysh oscillations which enabled an estimation of the electric-field strength of ~ 20 kV/cm at the sample surface. By analyzing the SPV spectra we have determined that a buried interface rather than the sample surface mainly governs the SPV effect. The DSPV spectra revealed sharp features associated with excitonic interband transitions which energies were found to be in a good agreement with those calculated including the nonparabolicity of the energy bands. The dependence of the exciton linewidth broadening on the well width and the quantum index has shown that an average half monolayer well width fluctuations is mostly predominant broadening mechanism for QWs thinner than 10 nm. The line broadening in lightly doped QWs, thicker than 10 nm, was found to arise from thermal broadening with the contribution from Stark broadening due to random electric fields of the ionized impurities in the structures. We finally consider the possible influence of strong internal electric fields, QW imperfections, and doping level on the operation of THz sensors fabricated using the studied structures. © *2005 American Institute of Physics.* [DOI: 10.1063/1.1978970]

I. INTRODUCTION

The increasing use of terahertz (THz) frequencies in various applications has stimulated considerable interest in the development of compact THz devices based on semiconductor nanostructures. The facilities of modern molecular-beam epitaxy (MBE) technology enable semiconductor quantum wells (QWs) to be engineered so that the carrier transitions in subbands can be used either to generate THz radiation by a quantum cascade scheme[1] or to detect THz frequencies, for instance, employing quantum well infrared photodetector (QWIP) approach.[2] The other way to proceed, which attracts much attention due to easier fabrication and lower costs, is to involve impurities in bulk semiconductors since their transitions also fall into THz frequency range. As an illustration of such a kind of detection it is worth mentioning the blocked-impurity band concept,[3] conversely, as an example of generator there are phosphorus or gallium impurities in silicon.[4] If a shallow impurity is placed in a QW, then its intersublevel transitions can be tuned in a controlled way to the desired THz frequency. It is advantageous to use δ doping as it prevents the extension of impurity energy levels resulting from any distribution of the dopant atoms along the growth direction of the QWs. The structures prepared in such a way seem to be very attractive for fabrication of the THz detectors and emitters.[5–7] In this respect, the Be δ-doped GaAs/AlAs multiple quantum well (MQW) system is of special interest as it gives the maximum possible confinement for the acceptor states in the valence band and, thus, the maximum possible tuning range for the dipole-allowed $1s$-$2p$ transition of the acceptor. Usually, such intraacceptor transitions are studied at low doping densities ($<3 \times 10^{16}$ cm^{-3}) to avoid impurity band effects smearing out the sharp absorption lines at higher concentrations.[8]

The effect of quantum confinement on the transitions of

[a)]Author to whom correspondence should be addressed; electronic mail: jk@pfi.lt

Be acceptors confined in GaAs/AlAs MQWs has already been investigated theoretically[9] and experimentally by far-infrared absorption[7,10] and photoluminescence[9,11] techniques. The data revealed important information about the binding energy and the carrier dynamics within the Be acceptor levels, in particular, the ability to alter the transition energy and the hole lifetime by the confinement potential of the QWs was demonstrated. However, the previous investigations were not extended to the spectral region of interband optical transitions, where excitons are expected to play a dominant role and can thus be used in the study and characterization of QW structures.[12] As is well known, the structural quality of QW structures is essential for the performance of semiconductor devices. Therefore, knowledge about the presence of internal electric fields, interface roughness, and other imperfections in δ-doped GaAs/AlAs structures is of particular importance for the technological development of far-infrared detectors and solid-state terahertz lasers.

Contactless and therefore nondestructive photoreflectance (PR) spectroscopy,[13,14] surface photovoltage (SPV) spectroscopy,[15] as well as differential SPV (Refs. 16 and 17) (DSPV) are especially attractive techniques for studying the optical and electronic properties of low-dimensional semiconductor structures. They offer the possibility of carrying out an investigation of quantum structures with high spectral sensitivity even at room temperature. Due to its high sensitivity, the PR technique has been widely used for the investigation of electronic structure and internal electric fields of various bulk semiconductors and heterostructures.[14] As a rule, the PR spectra of multilayer systems are very complicated due to the superposition of signals originating from separate regions, including surfaces and interfaces in the sample.[18] Therefore, a comparative study of QW structures by various optical characterization techniques, such as PR and DSPV spectroscopies is useful when interpreting the optical data.

In this work, we present a systematic study of room-temperature PR, SPV, and wavelength-modulated DSPV of optical interband transitions in Be δ-doped GaAs/AlAs MQW structures. Analyzing Franz-Keldysh oscillations (FKO) in PR spectra and the line shape of the DSPV allowed us to extract information on the built-in electric fields and the excitonic parameters for a large number of QW subbands, as well as the structural quality of the samples studied. The experimental optical transition energies were compared with calculations performed within the envelope function approximation taking into account nonparabolicity of the energy bands. The dominant exciton line broadening mechanisms were revealed and the interface roughness was evaluated from an analysis of the dependence of the exciton linewidth broadening on the QW width and the subband quantum number.

II. SAMPLES AND EXPERIMENT

A series of Be δ-doped GaAs/AlAs MQWs with the doping at the well center as well as a single epilayer of GaAs:Be was grown by MBE on a semi-insulating (100) GaAs substrate in a VG V80H reactor with all solid sources.

TABLE I. Characteristics of the samples: the repeated period, the quantum well width (L_w), the δ-doping Be concentration (N_A), and the growth temperature of the epitaxial layer (T).

Samples	Periods	L_w (nm)	N_A (cm^{-2})	T (°C)
1795	400	3	2×10^{10}	550
1794	200	10	5×10^{10}	550
1303	50	15	2.5×10^{12}	540
1392	40	20	2.5×10^{12}	540
1807	100	20	5×10^{10}	550
2068	300	5	5×10^{10}	550
2071	300	5	5×10^{12}	550
1796	5-μm-thick GaAs epilayer		2×10^{16} cm^{-3}	550

Prior to the growth of the MQW, a GaAs buffer layer of 300-nm thickness was grown. Each of the MQW structures investigated contained the same, 5-nm width AlAs barrier, while each GaAs well layer was δ doped at the well center with Be acceptor atoms. The structures were capped with a 100-nm GaAs layer. The doping level and the main characteristics of each sample are summarized in Table I. The schematic band diagram of δ-doped GaAs/AlAs MQW structures was calculated from Poisson's equation and it is shown in Fig. 1. It was assumed that the surface Fermi level for p-type GaAs is pinned at 0.5 eV above the valence band.[19] Consequently, this results in the formation of a surface depletion layer and a surface electric field. Another depletion layer is also formed at the interface between the MQW layer and the substrate due to Fermi-level pinning near the midgap of the semi-insulating GaAs.

The PR measurements were performed using a He–Ne 632.8-nm wavelength laser or a light-emitting diode (LED) (470-nm wavelength) as the modulation and/or continuous-wave illumination pump sources. The penetration depth of the He–Ne and LED light beams into GaAs were calculated to be about 250 and 50 nm, respectively. The PR spectra were measured in phase with the modulated 650-Hz pump beam. Pump intensities were kept below 2 mW cm^{-2}. The SPV measurements were performed in a chopped light geometry using a capacitorlike system with a transparent conducting top electrode[20] under normalized incident light intensity conditions. The illumination intensity was selected at sufficiently low levels in order not to affect the line shape of the spectra. In the DSPV spectrum measurements, a wavelength-modulation technique was used.[16,17] The wavelength of the incident probe light was modulated by vibrating
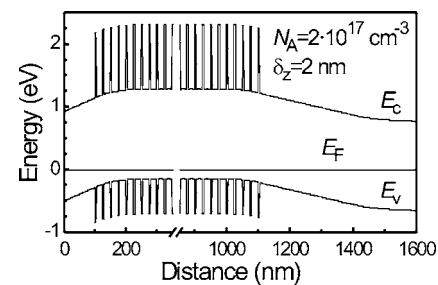

FIG. 1. Band diagram of δ-doped MQW structure. E_c and E_ν are the conduction- and valence-band edges. δ_z is the width of the Be-doped layer.
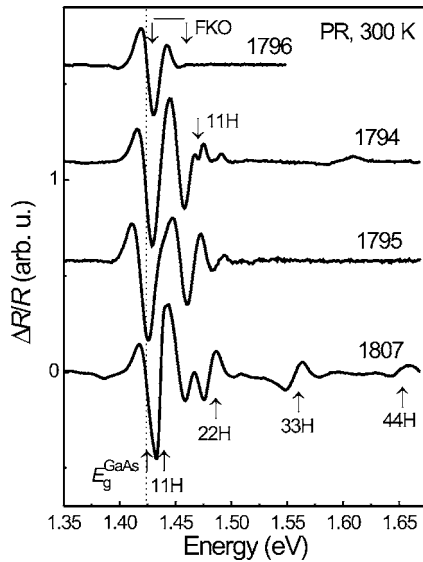
FIG. 2. Room-temperature PR spectra of GaAs epilayer 1796 and δ-doped GaAs/AlAs MQW samples with different well widths obtained with pumping He–Ne laser with a wavelength of 632.8 nm. The energies of optical transitions are marked by arrows. For convenience, the spectra obtained for the different samples are vertically shifted.

a fused-silica plate at 87 Hz located near the exit slit of the monochromator. The PR, SPV, and wavelength-modulated DSPV signals were recorded by a conventional lock-in detection system. The measurements were performed at room temperature.

III. RESULTS AND DISCUSSION

A. PR spectra

In Fig. 2 we present PR spectra in the region 1.35–1.70 eV for the GaAs/AlAs MQW samples with various well widths and doping concentrations. The PR spectrum from an epitaxial *p*-GaAs layer is also shown for comparison. By analyzing the spectra, we identified two sets of PR features related to various optical transitions in the MQW structure. Firstly, the PR features arising in the vicinity of the GaAs fundamental gap E_g (1.424 eV) with the characteristic oscillations are clearly observed in the PR spectra of the GaAs epilayer 1796 and GaAs/AlAs MQW samples 1794 and 1795. It should be noted that the oscillatory behavior of the PR signal above the band-gap energy of GaAs is not related to light interference fringes in the reflectivity spectra (they are not depicted). Furthermore, it was found that the PR oscillation period could be reduced by illumination (optical bias) due to the photovoltage effect. Therefore, these PR features were associated with FKOs indicating the existence of an internal electric field in the samples. Secondly, at higher energies, one can see a number of *mnH(L)* features related to optical transitions in the MQW region of the samples. The notation *mnH(L)* signifies the transitions between the *m*th electron and *n*th heavy-hole (*H*) or light-hole (*L*) subbands. The energies and broadening parameters of optical transitions responsible for observed PR features (Fig. 2) were determined from the fit of the PR spectra to the first derivative of a Lorentzian-type function proposed by

Aspnes[21] which is appropriate for excitonic transitions in QW structures.[13,14] The energies of the optical transitions, denoted by arrows in Fig. 2, were found to change according to the QW thickness as expected from the quantum confinement effect. For the large well width samples 1807, 1303, and 1392, the intense ground-state QW transitions occur rather close in energy to the GaAs band gap. Therefore, bulk-like FKO signals were not well resolved in the PR spectra of these samples.

First we discuss the origin of the FKO features above the GaAs band gap. According to the calculated band diagram (Fig. 1), the FKO features for the structures studied may originate from the photomodulation of the band bending near the surface, in the GaAs cap layer, and/or near the interface, in the GaAs buffer layer. Obviously, the effectiveness of the photomodulation of the interfacial electric field is limited due to light absorption in the structure above the buffer layer. Therefore, the PR intensity should be strongly dependent on the thickness of the structure as well as the wavelength (penetration depth) of the incident light.[13,14].

In the analysis of the internal electric-field strength, the oscillating behavior of FKOs is described as[22]

$$\frac{\Delta R}{R} \sim \cos\left\{\frac{4}{3}\left[\frac{E-E_g}{\hbar\theta}\right]^{3/2} + \varphi\right\}, \tag{1}$$

where E is the photon energy, E_g stands for the band-gap energy, $\hbar\theta = (e^2 F^2 \hbar^2/8\mu)^{1/3}$ denotes an electro-optic energy, e designates the electron charge, μ marks the reduced mass of the electron and hole in the direction of the electric field F, $\hbar$ labels Planck's constant, and φ is a phase factor which is influenced by any inhomogenity of the internal electric field.[23]

In addition, the phase of FKOs originating from the buried interface shifts strongly with the change of the epilayer thickness due to an interference effect.[24] We therefore used these peculiarities of the spectra to disclose the origin of FKOs. Let us consider in more detail the PR results for samples 1807, 1794, and 1795 given in Fig. 2. It can be seen that the change of the thickness of the MQW layer from 2.5 (sample 1807) to 3.2 μm (sample 1795) hardly affects the phase of the FKOs. Also, we found that the phase and the period of the FKOs do not depend on the wavelength (penetration depth) of the pump beams. Therefore, it could be inferred that the PR signals for these thick MQW samples arise mainly due to the photomodulation of the surface electric field. Consequently, taking into account the band diagram depicted in Fig. 1, these δ-doped structures should exhibit a nearly uniform electric field in the undoped GaAs cap layer and cause slowly decaying FKOs in the PR spectra. In contrast, due to broadening effects and the nonuniform electric field in a doped epitaxial GaAs layer, the FKOs are more heavily damped (Fig. 2). In accordance with Eq. (1), the built-in electric-field strength was evaluated by fast Fourier transform (FFT) analysis of the FKOs in the energy region above the GaAs band gap.[25] Prior to the Fourier analysis, the experimental PR spectrum has been renormalized substituting a new argument $(E-E_g)^{3/2}$ and multiplying the spectrum by $E^2(E-E_g)$ in order to deal with periodic functions and compensate for the damping of the FKOs, respectively.
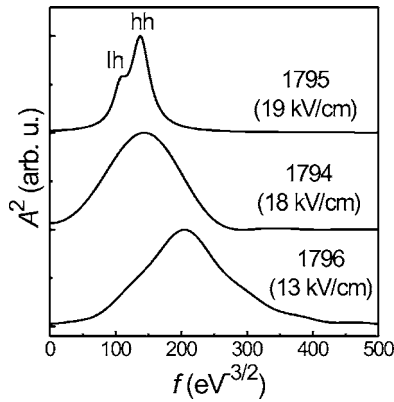
FIG. 3. Fourier transforms of the FKOs in the PR spectra (Fig. 2) for samples 1794, 1795, and 1796.

Then, according to Eq. (1), the peak quasifrequency f of the band in the spectrum, evaluated from the Fourier transform of the FKO, is related to the electric field by

$$f = \frac{2}{3\pi}(\hbar\theta)^{3/2} = \frac{4\sqrt{\mu}}{3\pi}\frac{1}{e\hbar F}. \tag{2}$$

The FFTs of the PR spectra of several of the GaAs/AlAs MQW structures are plotted in Fig. 3. For sample 1795, the two peaks of the FFT correspond to the heavy (hh) and light (lh) hole subband contributions to the PR spectra. The ratio of frequencies $f_{hh}/f_{lh}=1.29$ is consistent with the ratio[25] of $(\mu_{hh}/\mu_{lh})^{0.5}$. For other samples, only a single peak is seen in the transformed spectra arising from the more intense heavy-hole-related band-gap transition. These peaks are very broad due to the small number of FKOs in the PR spectra, and the signature of the light-hole contribution is not resolved. The calculated surface electric fields using Eq. (2) are also presented in Fig. 3. The electric-field values obtained in the cap layer of the MQW structures are about 20 kV/cm and are consistent with the calculated surface field value (Fig. 1) for an acceptor concentration of 2×10^{17} cm^{-3}.

B. SPV and DSPV spectra

1. Characteristic features

Figure 4 shows the SPV spectra of the different MQW samples measured under the same conditions. At low photon energies, all of these spectra exhibit a sharp increase in the photovoltage, which can be related to the onset of absorption in bulk GaAs layers. The shoulder around 1.39 eV in the spectra seems to be due to the impurities, while the knee at 1.42 eV is related to the GaAs band edge. At higher energies, pronounced discrete dips that could be associated with excitonic transitions in MQWs are clearly visible. It is an interesting characteristic that the spectra show n-type behavior (positive sign) in spite of the presence of p-type band bending near the surface. These results can be understood by taking into account the fact that two oppositely directed internal electric fields exist in the structures, one in the cap layer and another one in the buffer layer (see Fig. 1). In this case, the total SPV signal should be considered as a superposition of the two signal components with opposite sign.[15] As the total SPV is positive, it means that the SPV signal
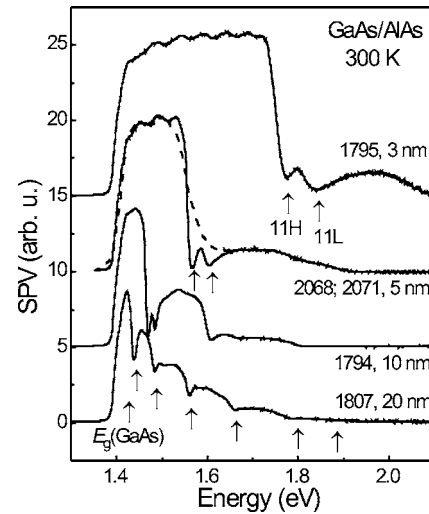

FIG. 4. Experimental SPV spectra of δ-doped GaAs/AlAs MQW structures at room temperature. The spectra are vertically shifted for clarity. The dashed curve represents data for sample 2071 (Table I). The interference pattern due to internal multiple reflections from the interfaces is visible below the exciton transitions edge 11H similarly to the reflectivity spectra. Note the absence of excitonic peaks and a step-like behaviour of SPV spectra originating from interband transitions in the highly doped sample 2071 (dash line).

component coming from the interface region of the GaAs buffer layer is very strong, and that it cancels the signal from the surface region. This is probably because the ratio of SPV signals from the surface and interface depletion regions should depend on the efficiencies of the generation and the spatial separation of electron-hole pairs. Since the GaAs cap layer is relatively thin, the SPV signal arises mostly due to light absorption in the GaAs buffer layer of the MQW sample. In addition, light absorption also takes place in the QWs. Consequently, it is very likely that the dips observed in the SPV spectra at the energies above the GaAs band gap arise mainly due to the attenuation of incident light passing through the MQW layer at the exciton resonances.[26] Therefore, the SPV spectra above the GaAs band-gap energy represent typical transmissionlike spectra of the MQW layer.

Further evidence for the origin of the SPV was provided by measurements of the edge-incident photovoltage spectra. We did not observed any QW-related features in these spectra. This rules out the possibility that the observed SPV features could be attributed solely to the photovoltage activity of MQWs themselves. The short electric-field penetration depth into the MQW region (Fig. 1), the relatively thick barriers preventing fast carrier tunneling, and the large recombination rate of any photocreated carriers in the doped QWs can account for the reduced photovoltaic activity of the MQW samples studied.

The interference pattern due to internal multiple reflections from the interfaces is also visible below the exciton transitions edge 11H (Fig. 4), just like in the reflectivity spectra. The minima in the SPV spectra correspond to maxima in the reflectivity spectra. The thickness d of the layer that produces light interference can be estimated by using the relationship $d=\lambda_1\lambda_2/2n_0(\lambda_1-\lambda_2)$, where n_0 is the refractive index, and λ_1 and λ_2 are the wavelengths of the
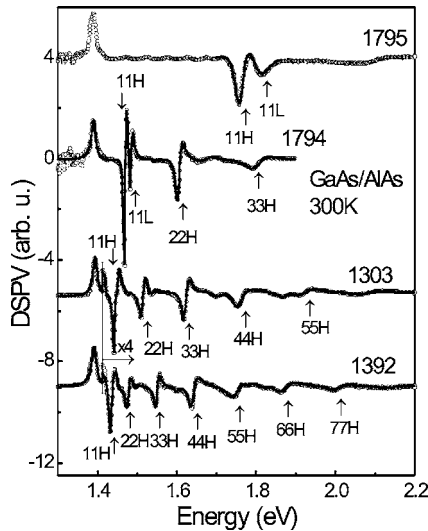
FIG. 5. Room-temperature wavelength-modulated DSPV spectra of δ-doped GaAs/AlAs MQW structures (open circles). The solid lines are least-squares fits to the first derivative of a Lorentzian-type function. Energies of the transitions are marked by arrows. The spectra obtained for the different samples are vertically shifted for clarity.

two adjacent maxima (or minima). For example, for sample 1795 using this procedure, we find that $d=3.4$ μm. This value is in good agreement with the nominal thickness of the MQW layer (3.2 μm) of this sample (Table I).

Note that excitonic peaks in the SPV spectra of the MQW samples are observed for the doping level $N_A \lesssim 2.5 \times 10^{12}$ cm^{-2}. If the doping density is increased to 5×10^{12} cm^{-2}, excitonic peaks disappear completely and a steplike behavior of SPV spectra originating from interband transitions is observed (Fig. 4, dashed line representing data for highly doped sample 2071). This change in the line shape of the SPV spectra probably occurs due to the screening of the excitons by free holes in the QWs.

In order to study the QW-related optical transitions with higher resolution, we have measured the DSPV spectra. The data for four GaAs/AlAs MQW samples are shown by open circles in Fig. 5. The excitonic features in the DSPV spectra were analyzed on the basis of the model assuming that normal-incident SPV features for MQWs are related to photoabsorption. We suppose that the spectral responsivity of the buried interface region above the GaAs band-gap energy is slowly varying with wavelength, compared to the sharp spectral lines of the optical transitions in the MQW. In this case, neglecting the spectral dependence of the reflectivity, the measured quantity dV/dE of the DSPV should be related to the first derivative of the absorption coefficient α of the MQW layer versus the photon energy E (Ref. 27)

$$\frac{1}{V}\frac{dV}{dE} \sim \frac{1}{d_w}\frac{1}{I}\frac{dI}{dE} = -\frac{d\alpha}{dE}, \tag{3}$$

where V is the SPV signal, d_w is the thickness of the MQW absorbing layer, and I is the light intensity absorbed in the GaAs buffer layer.

We found experimentally that the SPV amplitude above the GaAs band-gap energy increases linearly with the excitation intensity under weak illumination and tends to saturate at strong illumination. Therefore, for the regime of weak excitation, the wavelength dependence of the SPV above the GaAs band gap can be related to the spectral dependence of the absorption coefficient of the MQW layer. In this case the normalized DSPV, $(dV/dE)/V$, spectra are qualitatively equivalent to the first derivative of the absorption spectra.[27]

2. Optical transitions

The optical transitions in the GaAs/AlAs QWs were examined on the basis of a line-shape analysis of the normalized DSPV spectra. The spectra were fitted to the first derivative of a Lorentzian-type function.[21] As can be seen from Fig. 5, the experimental DSPV data (open circles) are reasonably well described by this line-shape model (lines). Moreover, the fit allows estimations of the optical transition energies (the arrows in Fig. 5) and the line broadening parameters.

To identify the spectroscopic data, we have carried out calculations of the energy levels and interband transition energies for GaAs/AlAs QWs for nonparabolic energy bands in the envelope function approximation using energy-dependent effective electron and light-hole masses.[28] At the conduction-band edge, the effective masses of the electrons are $m_e=0.0635m_0$ in GaAs and $m_e=0.15m_0$ in AlAs.[29] At the valence-band edge, the effective masses of the heavy and light holes along the z direction were evaluated from Luttinger parameters $\gamma_1=6.98$, $\gamma_2=2.06$ for GaAs and $\gamma_1=3.76$, $\gamma_2=0.82$ for AlAs.[29] The forbidden energy-gap values are $E_g^\Gamma=1.424$ and 3.018 eV for GaAs and AlAs, respectively.[30] The conduction-band offset was taken to be 0.65. In the calculations, we assumed that the QW potential profile is rectangular. To check this assumption, the calculations of energy levels by solving the coupled Poisson-Schrödinger equations have also been performed. It was found that the change in the ground-state optical transition energy due to distortion of the rectangular QW potential profile by δ doping is negligible and reaches only $\lesssim 3$ meV when the concentration of acceptors is 2.5×10^{12} cm^{-2} and the width of the QW is 20 nm. For narrower QWs and higher-order optical transitions the deviations were found to be even smaller.

The calculated interband transition energies for GaAs/AlAs QWs with the 5-nm AlAs barriers are plotted as a function of well width in Fig. 6. The exciton energies obtained from the analysis of the experimental DSPV spectra are also shown by symbols. As can be seen from Fig. 6, for most transitions studied the calculated interband energies exceed the experimental data by $\sim 3-10$ meV. This difference, which increases with decreasing QW thickness, should be equal to the exciton binding energy that was not included in our calculations. Indeed, it is somewhat smaller than the exciton binding energies in GaAs/AlAs QWs obtained from photoluminescence excitation studies.[31] Some decrease of exciton binding energies in our samples may be due to exciton screening by free holes in δ-doped QWs.[32]

3. Broadening mechanisms of the spectral lines

Now we shall discuss the spectral line broadening estimated from the DSPV and PR spectrum analysis. The well
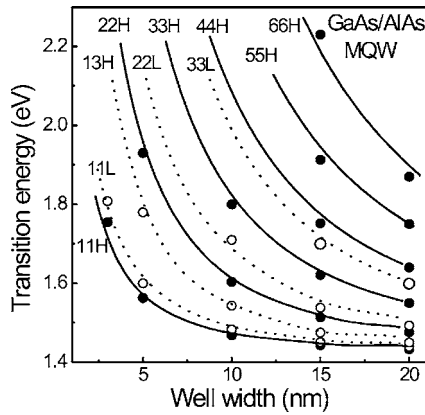
FIG. 6. Experimental (symbols) and calculated (lines) interband transition energies vs well widths for δ-doped GaAs/AlAs MQWs. The solid symbols and solid lines, open symbols and dotted lines represent allowed heavy-hole-related transitions, mnH, and light-hole-related allowed transitions, mnL, respectively. Weakly allowed 13H transition is depicted by open symbols and dashed line, too.

FIG. 8. The evolution of the broadening parameters of heavy-hole excitons related optical transitions as a function of the quantum number n in δ-doped GaAs/AlAs MQWs with different well widths.

width dependence of the broadening parameter Γ which represents the full width at half maximum (FWHM) of the exciton line for 11H optical transitions is shown by symbols in Fig. 7. As can be seen, for thin QWs ($L_w \leqslant 10$ nm), a rapid rise in the linewidth up to about 35 meV is observed with decreasing QW thickness from 10 to 3 nm. On the other hand, for thick QWs ($L_w \geqslant 10$ nm), where Γ is equal to about 10 meV, it practically does not change with L_w or even tends to increase slightly with increasing well width up to 20 nm. This tendency arises mainly from the fact that the Γ values for highly doped samples (solid symbols) are found to be somewhat larger than those for lightly doped ones (open symbols).

In analyzing the experimental $\Gamma(L_w)$ dependencies, several linewidth broadening mechanisms should be considered:[33] (i) thermal broadening (Γ_{th}) due to phonon scattering, (ii) inhomogeneous broadening of the exciton energy levels (Γ_{inh}) caused by structural imperfections in QWs,
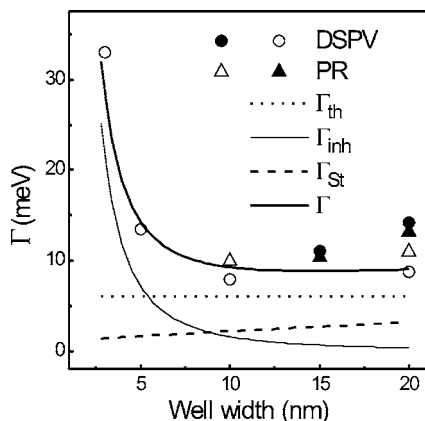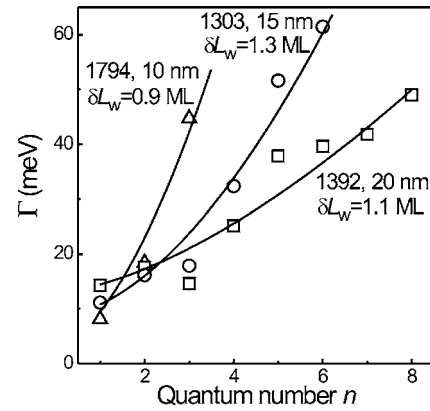
such as interface roughness or composition fluctuations in the alloy, (iii) broadening due to the Stark effect in nonuniform internal electric fields (Γ_{St}), and (iv) linewidth broadening due to band filling or exciton scattering by free carriers (Γ_c).

Considering the experimental $\Gamma(L_w)$ data from the point of view of thermal broadening, we used the value of $\Gamma_{th} = 6$ meV (Fig. 7, dotted line). This number was estimated from the study of the temperature dependence of exciton scattering by longitudinal-optical and acoustic phonons in GaAs/AlGaAs QWs.[34,35]

The inhomogeneous linewidth broadening Γ_{inh} (FWHM) due to well width fluctuations was evaluated as the change of exciton energy E_n with the variation of the well width,[12]

$$\Gamma_{inh}(n) = 2.36 \frac{dE_n}{dL_w} \delta L_w, \qquad (4)$$

where δL_w is the standard deviation of the well width fluctuations which were assumed to obey a Gaussian distribution and n is the quantum number of the QW subbands.

As may be seen from Fig. 6, the differential energy shift dE_n/dL_w grows with increasing quantum number n. Therefore, the well width fluctuations δL_w in thick QWs, where ground-state optical transitions with $n=1$ are insensitive to a variation in L_w (Figs. 6 and 7), were evaluated from the experimental dependence of $\Gamma(n)$ (Fig. 8). The experimental data $\Gamma(n)$ were analyzed by the relation $\Gamma(n) = a + \Gamma_{inh}(n)$ where the parameter a was assumed to include homogeneous broadening contributions and $\Gamma_{inh}(n)$ was calculated using Eq. (4). In these considerations, the δL_w and a were treated as adjustable parameters while the derivatives dE_n/dL_w were calculated taking into account the nonparabolicity of the energy bands. In this way, the average well width fluctuations δL_w in thick QWs were found to be equal to 0.9–1.3 monolayers (MLs) which in GaAs corresponds to 2.83 Å.

The well width fluctuations in narrow QWs were estimated by analyzing the Γ dependence on L_w for the ground-state excitonic transitions. The data are shown in Fig. 7. Before proceeding to a more detailed discussion on these results, it is worth noting the following. In order to perform such an analysis, the exciton line Stark broadening Γ_{St}, caused by the internal electric fields in MQW structures,

FIG. 7. Experimental (symbols) and calculated (thick solid curve) broadening parameter Γ (FWHM) of 11H excitonic transitions in δ-doped GaAs/AlAs MQWs as a function of the well width L_w. In addition, we have plotted the calculated contributions to the linewidth broadening due to well width fluctuations Γ_{inh} (thin solid curve), exciton interaction with phonons Γ_{th} (dotted line), and broadening induced by random electric fields of ionized impurities Γ_{St} (dashed curve).

should be evaluated. This is a rather complicated problem as the spectral line broadening Γ_{St} can arise from the Stark effect in a random Coulomb field of ionized impurities in δ-doped planes, in nonuniform surface and interface electric fields and, also, in electric fields caused by well-to-well fluctuations in doping.[33,36] If the Γ_{St} originates mainly from the Coulomb fields of ionized impurities, it can be expressed as[36]

$$\Gamma_{St} \approx 2 \times 10^{-30} N_i^{4/3} \left(\frac{m_0}{\mu}\right)^2 E_b^{-1}, \qquad (5)$$

where N_i is the concentration of ionized impurities, E_b is the exciton binding energy, m_0 is the free electron mass, and μ is the reduced electron-heavy-hole mass.

Therefore, including various broadening mechanisms, the total $\Gamma(L_w)$ dependence was calculated as $\Gamma = \Gamma_{th} + \Gamma_{inh} + \Gamma_{St}$. The experimental data for lightly doped QWs (Fig. 7, open symbols) were fitted reasonably by choosing $\delta L_w = 0.5$ ML (Fig. 7, a thin solid curve representing Γ_{inh}) and $N_i = 10^{17}$ cm^{-3} (Fig. 7, a dashed curve representing Γ_{St}). By calculating Γ_{St}, the exciton binding energies from Ref. 31 were employed. It should be noted that using the values determined above $\delta L_w \approx 1$ ML for thick QWs does not have a significant influence on the results of the analysis because, according to Eq. (4), a 1-ML fluctuation in a 20-nm well width causes about a 0.8-meV fluctuation in the transition energy. Further, one may suppose that smaller δL_w values estimated in narrow QWs as compared to the thick ones can be due to the correlation effects of well width fluctuations in narrow QWs.[37] Note also the spectroscopically obtained concentration of ionized impurities $N_i \lesssim 10^{17}$ cm^{-3} corresponds to an areal density of approximately $\sim 2 \times 10^{10}$ cm^{-2} (assuming the diffusion length of 2 nm).

By examining the $\Gamma(L_w)$ dependence, the exciton line broadening due to scattering by free carriers was also considered. According to Shen *et al.*,[38] it has been evaluated that at a carrier density equal to 2×10^{10} cm^{-2} the spectral line broadening should be $\lesssim 0.2$ meV. However, this component should increase linearly with two-dimensional (2D) carrier density and could be taken into account by explaining exciton line broadening in highly doped samples.

Thus, the analysis performed on the exciton linewidth broadening in δ-doped GaAs/AlAs MQW structures indicate that in narrow QWs the dominant mechanism is the well width fluctuations. In thick QWs, phonon and Stark broadening due to random electric fields was found to be predominant.

Before we proceed to the conclusions, it is reasonable to briefly consider the relevance of the information obtained concerning the structural properties and inherent features of studied MQWs with respect to the design of the THz sensors. It is worth noting that very recently we have fabricated and tested the THz sensors based on the studied GaAs/AlAs MQWs. Terahertz photocurrent, measured along the QWs layers, has shown that such devices can operate within 5.4–7.3 THz frequency range at low temperatures.[39] The main mechanism responsible for the photocurrent signal was assumed to be photothermal ionization of Be acceptors. Although the optical data reveal the presence of strong internal electrical fields and some imperfections of different origin in

the structures, one can deduce that these features seem not to be a serious obstacle for the realization of THz detectors. We should emphasize, however, that in designing such devices the effect of doping should be also taken into account: in interband spectra these effects appear in the quenching of excitonic lines and the increase of broadening parameter with higher doping density. Meanwhile, in the THz range, it could bring about a redshift of detection frequency.[39]

We conclude that Be-doped GaAs/AlAs structures could serve as an active component creating a new type of THz sensor which relies on *in-plane* carrier transport in doped QWs, in contrast to the QWIP type of devices where carrier movement *perpendicular* to QW layers is responsible for device operation.

IV. CONCLUSIONS

In summary, room-temperature PR, SPV, and DSPV spectra of Be δ-doped GaAs/AlAs MQW structures designed for THz sensing applications have been measured. The excitonic interband transitions and the structural quality of the samples were examined with QW widths ranging from 3 to 20 nm and doping level varying from 2×10^{10} to 5×10^{12} cm^{-2}. It has been demonstrated that the nondestructive PR, SPV, and DSPV methods can give valuable information about internal electric fields, electronic structure, and broadening of excitonic resonances in δ-doped MQWs.

The surface electric-field strength estimated by FFT analysis of FKO in the PR spectra was found to be ~ 20 kV/cm. We discussed the origin of the SPV signal in the MQW samples and revealed that a dominant SPV component comes from the GaAs buffer layer. Also, it was found that features in the SPV and DSPV spectra exhibit excitonic behavior showing that doping effects are not critical for the observation of excitonic transitions at the acceptor densities up to 2×10^{12} cm^{-2}. From the line-shape analysis of the PR and DSPV spectra the exciton transition energies and linewidth broadening parameters for a large number of QW-related transitions were determined. The spectroscopic data of transition energies are found to be in agreement with calculations performed within the envelope function approximation which took into account the nonparabolicity of the energy bands.

Analysis of the dependence of the exciton linewidth broadening on the subband quantum number and the QW width allowed to evaluate line broadening mechanisms and interface roughness in the MQW structures. It was found that in QWs thinner than 10 nm the dominant line broadening mechanism is from the average half-ML well width fluctuations. In QWs thicker than 10 nm, the average well width fluctuations are found to be ~ 1 ML. Also, in lightly doped thick QWs, where the exciton line is insensitive to interface roughness, the linewidth was explained mainly by thermal and Stark broadening due to the random electric fields of ionized impurities. We observed a trend of an increasing broadening parameter with increasing doping density. This may be due to enhanced exciton scattering by ionized impurities and free holes. However, to evaluate the effect of doping on exciton line broadening, more detailed studies of the

dependence of the modulation spectra of GaAs/AlAs MQWs on the Be acceptor density are needed. Finally, it was concluded that the presence of strong internal electric fields and QW imperfections must be taken into account in designing THz sensors based on the studied structures.

ACKNOWLEDGMENTS

[1] R. Köhler *et al.*, Nature (London) **417**, 156 (2002); B. S. Williams, H. Callebaut, S. Kumar, Q. Hu, and J. L. Reno, Appl. Phys. Lett. **82**, 1015 (2003); L. Ajili, G. Scalari, J. Faist, H. Beere, E. Linfield, D. Ritchie, and G. Davies, *ibid.* **85**, 3986 (2004).

[2] M. Graf, G. Scalari, D. Hofstetter, J. Faist, H. Beere, E. Lindfield, D. Ritchie, and G. Davis, Appl. Phys. Lett. **84**, 475 (2004); C. Liu, C. Y. Song, A. J. SpingThorpe, and J. C. Cao, *ibid.* **84**, 4068 (2004).

[3] I. C. Wu, J. W. Beeman, P. N. Luke, W. L. Hansen, and E. E. Haller, Appl. Phys. Lett. **58**, 1431 (1991).

[4] P.-C. Lv, R. T. Troeger, T. N. Adam, S. Kim, J. Kolodzey, I. N. Yassievich, M. A. Odnoblyudov, and M. S. Kagan, Appl. Phys. Lett. **85**, 22 (2004); P.-C. Lv *et al.*, *ibid.* **85**, 3660 (2004).

[5] P. Harrison, M. P. Halsall, and W.-M. Zheng, Mater. Sci. Forum **384–385**, 165 (2002).

[6] P. Harrison and R. W. Kelsall, J. Appl. Phys. **81**, 7135 (1997).

[7] M. P. Halsall, P. Harrison, J.-P. Wells, I. V. Bradley, and H. Pellemans, Phys. Rev. B **63**, 155314 (2001).

[8] R. A. Lewis, T. S. Cheng, M. Henini, and J. M. Chamberlain, Phys. Rev. B **53**, 12829 (1996).

[9] W. M. Zheng, M. P. Halsall, P. Harmer, P. Harrison, and M. J. Steer, J. Appl. Phys. **92**, 6039 (2002).

[10] W. M. Zheng, M. P. Halsall, P. Harrison, J.-P. R. Wells, I. V. Bradley, and M. J. Steer, Appl. Phys. Lett. **83**, 3719 (2003).

[11] W. M. Zheng, M. P. Halsall, P. Harmer, P. Harrison, and M. J. Steer, Appl. Phys. Lett. **84**, 735 (2004).

[12] K. K. Bajaj, Mater. Sci. Eng., R. **34**, 59 (2001).

[13] O. J. Glembocki and B. V. Shanabrook, *Semiconductors and Semimetals*, edited by D. G. Seiler and C. L. Littler (Academic, San Diego, 1992), Vol. 36, p. 221.

[14] F. H. Pollak and H. Shen, Mater. Sci. Eng., R. **10**, 275 (1993).

[15] L. Kronik and Y. Shapira, Surf. Sci. Rep. **39**, 1 (1999).

[16] Yu. Kavalyauskas, G. Krivaite, A. Shileika, L. V. Sharonova and Yu. V. Shmartsev, Semiconductors **27**, 598 (1993).

[17] J. S. Liang *et al.*, J. Appl. Phys. **93**, 1874 (2003).

[18] A. J. Shields and P. C. Klipstein, Phys. Rev. B **43**, 9118 (1991).

[19] S. M. Sze, *Physics of Semiconductors Devices*, 2nd ed. (Wiley, New York, 1981), Chap. 5.

[20] S. Datta, S. Ghosh, and B. M. Arora, Rev. Sci. Instrum. **72**, 177 (2001).

[21] D. E. Aspnes, Surf. Sci. **37**, 418 (1973).

[22] D. E. Aspnes and A. A. Studna, Phys. Rev. B **7**, 4605 (1973).

[23] D. E. Aspnes, Phys. Rev. B **10**, 4228 (1974).

[24] H. Takeuchi, Y. Yamamoto, R. Hattori, T. Ishikawa, and M. Nakayama, Jpn. J. Appl. Phys., Part 1 **42**, 6772 (2003).

[25] D. P. Wang and C. T. Chen, Appl. Phys. Lett. **67**, 2069 (1995).

[26] P. Blood, J. Appl. Phys. **58**, 2288 (1985).

[27] R. Braunstein, P. Schreiber, and M. Welkowsky, Solid State Commun. **6**, 627 (1968).

[28] V. Karpus, *Two-Dimensional Electrons* (Ciklonas, Vilnius, 2004).

[29] I. Vurgaftman, J. R. Meyer and L. R. Ram-Mohan, J. Appl. Phys. **89**, 5815 (2001).

[30] S. Adachi, J. Appl. Phys. **58**, R1 (1985).

[31] M. Gurioli, J. Martinez-Pastor, M. Colocci, A. Bosacchi, S. Franchi, and L. C. Andreani, Phys. Rev. B **47**, 15755 (1993).

[32] J. P. Loehr and J. Singh, Phys. Rev. B **42**, 7154 (1990).

[33] F. J. Stevens, M. Whitehead, G. Parry, and K. Woodbridge, IEEE J. Quantum Electron. **24**, 2007 (1988).

[34] A. Venu Gopal, R. Kumar, A. S. Vengurlekar, A. Bosacchi, S. Franchi, and L. N. Pfeiffer, J. Appl. Phys. **87**, 1858 (2000).

[35] A. Thranhardt, C. Ell, S. Mosor, G. Rupper, G. Khitrova, H. M. Gibbs, and S. W. Koch, Phys. Rev. B **68**, 035316 (2003).

[36] N. Dai, F. Brown, R. E. Doezema, S. J. Chuang, and M. B. Santos, Phys. Rev. B **63**, 115321 (2001).

[37] I. V. Ponomarev, L. I. Deych, and A. A. Lisyanski, Appl. Phys. Lett. **85**, 2496 (2004).

[38] W. Z. Shen, L. F. Jiang, K. Wang, and H. Z. Wu, J. Appl. Phys. **91**, 6507 (2002).

[39] B. Čechavičius, J. Kavaliauskas, G. Krivaitė, D. Seliuta, E. Širmulis, J. Devenson, G. Valušis, B. Sherliker, M. P. Halsall, M. J. Steer, and P. Harrison, Acta Phys. Pol. A **107**, 328 (2005).